Supporting Information

Anionic Modification of the Cu-Tb Single-Molecule Magnets Based on the Compartmental Schiff-Base Ligand

JI Wen-Jie, XIA Cheng-Cai, ZHANG Xin-Yu, WANG Xin-Yi*

(State Key Laboratory of Coordination Chemistry,
School of Chemistry and Chemical Engineering, Nanjing University, Nanjing 210023, China)

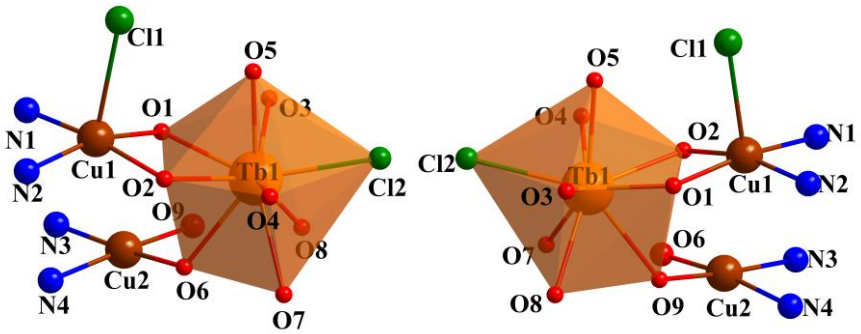

Figure.S1 The coordination environments of the meal centers in compounds **1** and **2**

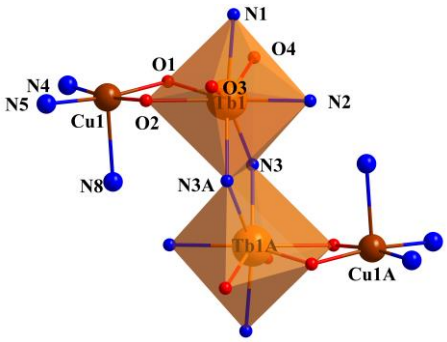

Figure.S2 The coordination environments of the metal centers in compound **3** (A = 1-x, 1-y, 1-z)

Table S1 Selected bond angles (°) for complexes 1-3

1		2		3	
Cl2-Tb1-O4	76.48(4)	Cl2-Tb1-O3	77.57(11)	O2-Tb1-O3	61.45(18)
O6-Tb1-Cl2	138.35(5)	O7-Tb1-Cl2	79.30(13)	O2-Tb1-O4	123.82(18)

O6-Tb1-O7	61.77(6)	O7-Tb1-O9	72.70(17)	O2-Tb1-N1	91.0(2)
O6-Tb1-O3	107.56(6)	O7-Tb1-O3	134.59(16)	O2-Tb1-N3^{A}	118.2(2)
O6-Tb1-O4	105.36(6)	O7-Tb1-O4	68.62(17)	O2-Tb1-N3	81.5(2)
O7-Tb1-Cl	83.33(5)	O7-Tb1-O8	74.42(17)	O1-Tb1-O2	65.55(19)
O7-Tb1-O3	141.40(7)	O7-Tb1-O5	139.19(18)	O1-Tb1-O3	122.62(18)
O7-Tb1-O4	65.19(6)	O9-Tb1-Cl2	141.78(12)	O1-Tb1-O4	60.68(19)
O8-Tb1-Cl2	78.78(5)	O9-Tb1-O3	104.34(14)	O1-Tb1-N1	88.6(2)
O8-Tb1-O6	70.85(7)	O9-Tb1-O4	109.96(14)	O1-Tb1-N3	118.8(2)
O8-Tb1-O7	74.47(7)	O9-Tb1-O8	62.26(14)	O1-Tb1-N3^{A}	85.3(2)
O8-Tb1-O3	67.18(7)	O2-Tb1-Cl2	140.66(12)	O3-Tb1-O4	145.07(18)
O8-Tb1-O4	134.46(6)	O2-Tb1-O7	100.27(16)	N1-Tb1-O3	72.3(2)
O8-Tb1-O5	136.72(7)	O2-Tb1-O9	71.11(15)	N1-Tb1-O4	73.1(2)
O1-Tb1-Cl2	143.52(5)	O2-Tb1-O1	66.22(15)	N1-Tb1-N3	144.4(3)
O1-Tb1-O6	71.78(6)	O2-Tb1-O3	122.13(15)	N1-Tb1-N3^{A}	143.9(3)
O1-Tb1-O7	132.28(6)	O2-Tb1-O4	61.77(15)	N2-Tb1-O2	146.5(3)
O1-Tb1-O8	101.01(6)	O2-Tb1-O8	132.59(15)	N2-Tb1-O1	146.9(3)
O1-Tb1-O2	64.95(6)	O2-Tb1-O5	76.17(16)	N2-Tb1-O3	85.5(3)
O1-Tb1-O3	62.25(6)	O1-Tb1-Cl2	133.54(11)	N2-Tb1-O4	86.3(3)
O1-Tb1-O4	121.39(6)	O1-Tb1-O7	143.05(17)	N2-Tb1-N1	83.9(3)
O1-Tb1-O5	76.35(7)	O1-Tb1-O9	70.39(15)	N2-Tb1-N3^{A}	82.1(3)
O2-Tb1-Cl2	133.05(5)	O1-Tb1-O3	58.81(14)	N2-Tb1-N3	83.6(3)
O2-Tb1-O6	72.88(7)	O1-Tb1-O4	123.59(15)	N3^{A}-Tb1-O3	138.9(2)
O2-Tb1-O7	90.48(7)	O1-Tb1-O8	89.72(16)	N3-Tb1-O3	73.5(2)
O2-Tb1-O8	143.66(7)	O1-Tb1-O5	73.44(17)	N3-Tb1-O4	138.9(2)
O2-Tb1-O3	123.35(6)	O4-Tb1-Cl2	82.37(11)	N3^{A}-Tb1-O4	72.9(2)
O2-Tb1-O4	59.03(6)	O4-Tb1-O3	143.89(15)	N3-Tb1-N3^{A}	66.2(4)
O2-Tb1-O5	75.08(7)	O8-Tb1-Cl2	85.69(11)	O2-Tb1-O3	61.45(18)
O3-Tb1-Cl2	85.15(4)	O8-Tb1-O3	65.37(15)	O2-Tb1-O4	123.82(18)
O3-Tb1-O4	145.74(6)	O8-Tb1-O4	142.63(16)	O2-Tb1-N1	91.0(2)
O5-Tb1-Cl	79.43(5)	O5-Tb1-Cl2	79.20(13)	O2-Tb1-N3^{A}	118.2(2)
O5-Tb1-O6	141.91(7)	O5-Tb1-O9	138.47(16)		
O5-Tb1-O7	138.60(7)	O5-Tb1-O3	72.49(16)		
O5-Tb1-O3	74.10(7)	O5-Tb1-O4	74.46(17)		
O5-Tb1-O4	74.26(7)	O5-Tb1-O8	137.37(16)	**(N3^{A}, A = 1-x, 1-y, 1-z)**	

Table S2 Continuous Shape Measures (CShMs) of the coordination geometry for Tb^{III} ion in compounds 1–3 calculated with the Shape program. The CShM values indicated the proximity to the ideal polyhedron, thus, CShM = 0 corresponds to the non-distorted polyhedron.

1		**2**		**3**	
polyhedron	CShM	polyhedron	CShM	polyhedron	CShM
HBPY-9 (D_{7h})	17.353	HBPY-9 (D_{7h})	18.827	HBPY-8 (D_{6h})	16.028
JTC-9 (C_{3v})	16.736	JTC-9 (C_{3v})	16.719	CU-8 (O_h)	15.687

JCCU-9 (C_{4v})	9.363	JCCU-9 (C_{4v})	9.977	SAPR-8 (D_{4d})	5.347
CCU-9 (C_{4v})	8.356	CCU-9 (C_{4v})	9.132	TDD-8 (D_{2d})	3.974
JCSAPR-9 (C_{4v})	2.562	JCSAPR-9 (C_{4v})	2.432	JGBF-8 (D_{2d})	11.625
CSAPR-9 (C_{4v})	1.802	CSAPR-9 (C_{4v})	1.793	JETBPY-8 (D_{3h})	23.639
JTCTPR-9 (D_{3h})	3.635	JTCTPR-9 (D_{3h})	3.260	JBTPR-8 (C_{2v})	2.832
TCTPR-9 (D_{3h})	2.491	TCTPR-9 (D_{3h})	2.383	BTPR-8 (C_{2v})	2.765
JTDIC-9 (C_{3v})	13.529	JTDIC-9 (C_{3v})	13.878	JSD-8 (D_{2d})	4.888
HH-9 (C_{2v})	9.762	HH-9 (C_{2v})	10.394	TT-8 (T_d)	16.071
MFF-9 (C_s)	1.054	MFF-9 (C_s)	0.981	ETBPY-8 (D_{3h})	22.047

(HBPY-9 (D_{7h}) = Heptagonal bipyramid, HBPY-8 (D_{6h}) = Hexagonal bipyramid,
JTC-9 (C_{3v}) = Johnson triangular cupola J3, CU-8 (O_h) = Cube,
JCCU-9 (C_{4v}) = Capped cube J8, SAPR-8 (D_{4d}) = Square antiprism,
CCU-9 (C_{4v}) = Spherical-relaxed capped cube, TDD-8 (D_{2d}) = Triangular dodecahedron,
JCSAPR-9 (C_{4v}) = JCSAPR-9, JGBF-8 (D_{2d}) = Johnson gyrobifastigium J26,
CSAPR-9 (C_{4v}) = Spherical capped square antiprism, JETBPY-8 (D_{3h}) = Johnson elongated triangular bipyramid J14,
JTCTPR-9 (D_{3h}) = Tricapped trigonal prism J51, JBTPR-8 (C_{2v}) = Biaugmented trigonal prism J50,
TCTPR-9 (D_{3h}) = Spherical tricapped trigonal prism, BTPR-8 (C_{2v}) = Biaugmented trigonal prism,
JTDIC-9 (C_{3v}) = Tridiminished icosahedron J63, JSD-8 (D_{2d}) = Snub diphenoid J84,
HH-9 (C_{2v}) = Hula-hoop, TT-8 (T_d) = Triakis tetrahedron,
MFF-9 (C_s) = Muffin), ETBPY-8 (D_{3h}) = Elongated trigonal bipyramid)

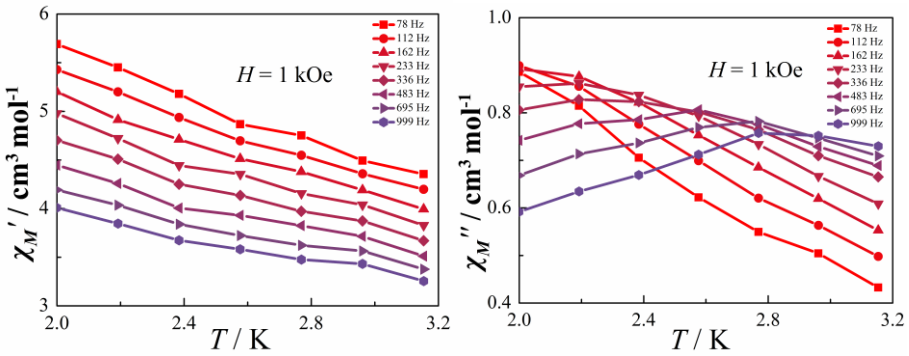

Figure.S3 Temperature dependence of in-phase (χ′) ac and out-of-phase(χ″) susceptibility signals for complex **1** under a 1000 Oe dc field

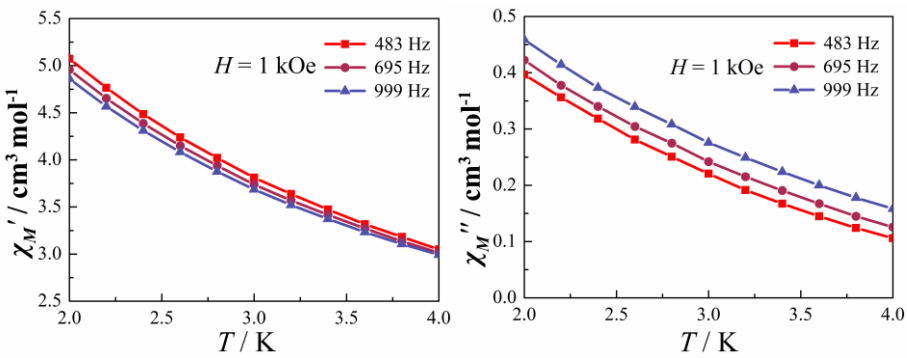

Figure.S4 Temperature dependence of in-phase (χ′) ac and out-of-phase(χ″) susceptibility signals for complex **2** under a 1000 Oe dc field

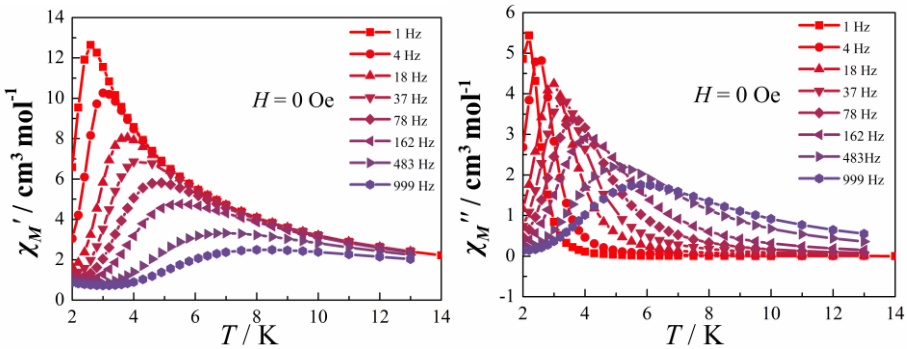

Figure.S5 Temperature dependence of in-phase (χ′) ac and out-of-phase(χ″) susceptibility signals for complex **3** under a 1000 Oe dc field

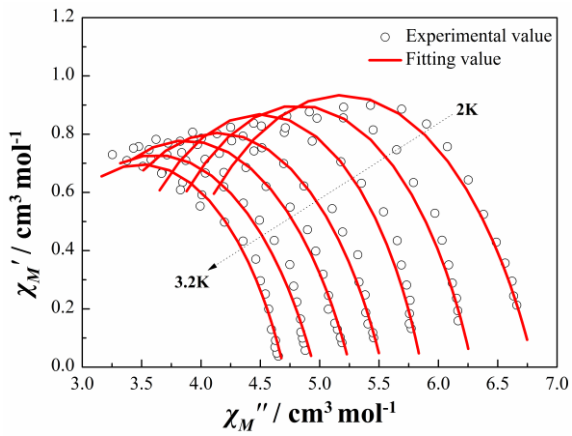

Figure.S6 Cole–Cole (Argand) plots for **1** obtained using the ac susceptibility data. The solid lines correspond to the best fit obtained with a generalized Debye model under an applied dc field

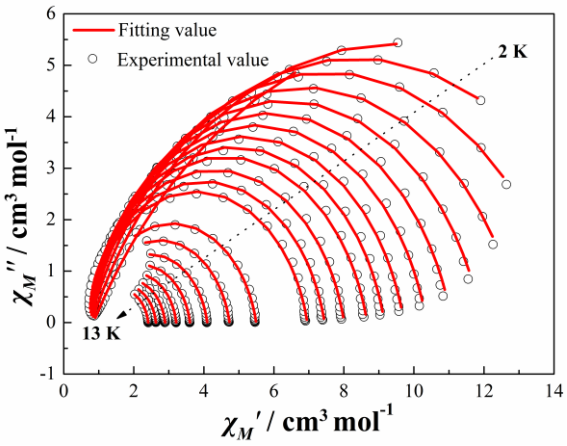

Figure.S7 Cole–Cole (Argand) plots for **3** obtained using the ac susceptibility data. The solid lines correspond to the best fit obtained with a generalized Debye model under a zero dc field

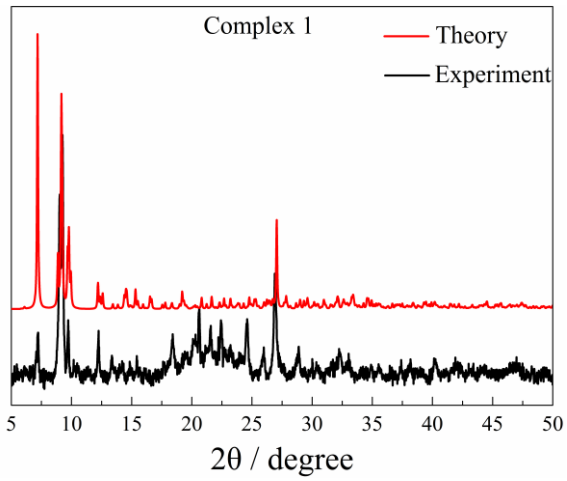

Figure.S8 X-ray powder diffraction pattern of complex **1** at room temperature, together with the calculated pattern from the single crystal data

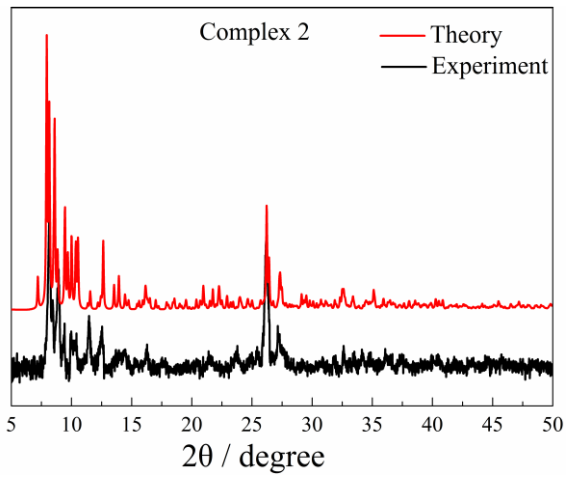

Figure.S9 X-ray powder diffraction pattern of complex **2** at room temperature, together with the

calculated pattern from the single crystal data

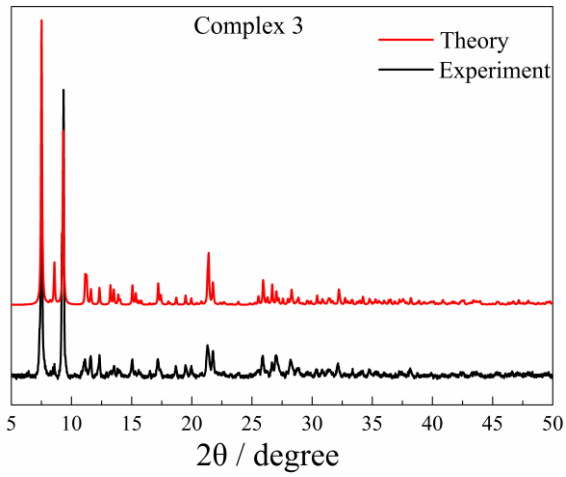

Figure.S10 X-ray powder diffraction pattern of complex **3** at room temperature, together with the calculated pattern from the single crystal data

Table S3 Best fitted parameters (χ_T, χ_S, τ, and α) with the extended Debye model for compound 1 under a 1000 Oe dc field in the temperature range of 2–3.2 K.

Temperature/K	χ_S / cm^3 mol^{-1} K	χ_T / cm^3 mol^{-1} K	τ / s	α
2	3.56191	6.80614	0.00101	0.33492
2.2	3.35141	6.28584	8.0047×10^{-4}	0.30027
2.4	3.13662	5.85833	6.8564×10^{-4}	0.27686
2.6	2.75614	5.52734	4.7883×10^{-4}	0.33027
2.8	2.48304	5.25722	3.6519×10^{-4}	0.34906
3	2.28568	4.95312	2.7714×10^{-4}	0.36333
3.2	2.29813	4.69559	3.0272×10^{-4}	0.33

Table S4 Best fitted parameters (χ_T, χ_S, τ, and α) with the extended Debye model for compound 1 under a zero field in the temperature range of 2–13 K.

Temperature/K	χ_S / cm^3 mol^{-1} K	χ_T / cm^3 mol^{-1} K	τ / s	α
2	0.84419	20.9938	0.46526	0.34697
2.2	0.78329	18.0646	0.15621	0.28727
2.4	0.7313	15.9457	0.06424	0.2438
2.6	0.69463	14.3527	0.03103	0.21187
2.8	0.65675	13.0351	0.01632	0.18991
3	0.64342	11.9505	0.00971	0.17009
3.2	0.62819	11.0856	0.00623	0.158
3.4	0.61525	10.358	0.00424	0.15073
3.6	0.60436	9.71575	0.00301	0.14574
3.8	0.59449	9.15766	0.00223	0.14317
4	0.58555	8.66166	0.0017	0.14219

4.3	0.58504	8.0081	0.00119	0.14083
4.6	0.5888	7.44817	8.7543×10^{-4}	0.14094
4.9	0.60242	6.95237	6.7116×10^{-4}	0.13956
5.2	0.60243	6.95237	6.7116×10^{-4}	0.13956
6.1	0.70142	5.4926	3.1318×10^{-4}	0.13698
7	0.78522	4.73356	2.1674×10^{-4}	0.13241
8	0.87233	4.09648	1.6329×10^{-4}	0.1245
9	0.924	3.60259	1.3309×10^{-4}	0.1164
10	0.95629	3.21143	1.1401×10^{-4}	0.10942
11	0.94428	2.89478	9.9678×10^{-5}	0.10727
12	0.95053	2.63144	9.0594×10^{-5}	0.10156
13	0.91724	2.41155	8.1232×10^{-5}	0.10179